Energy Reports 7 (2021) 2436–2451

Contents lists available at ScienceDirect

Energy Reports

journal homepage: www.elsevier.com/locate/egyr

Research paper

Comprehensive evaluation of flat plate and parabolic dish solar collectors' performance using different operating fluids and MWCNT nanofluid in different climatic conditions

Ping Ouyang [a,*,1], Yi-Peng Xu [b,1], Lu-Yu Qi [c,1], Si-Ming Xing [a], Hadi Fooladi [d]

[a] Engineering Research Center for Waste Oil Recovery Technology and Equipment, Ministry of Education, Chongqing Technology and Business University, Chongqing, 400067, China
[b] School of Mathematical Sciences, Tiangong University, Tianjin, 300387, China
[c] School of Electronic and Information Engineering, Tiangong University, Tianjin, 300387, China
[d] Department of Energy Engineering, Faculty of Engineering, Tabriz Branch, Islamic Azad University, Tabriz, Iran

ARTICLE INFO

Article history:
Received 25 November 2020
Received in revised form 2 April 2021
Accepted 23 April 2021
Available online 28 April 2021

Keywords:
Flat plate collector
Parabolic dish collector
Water and Dowtherm Q
MWCNT nanoparticle
Enviroeconomic and exergoenviroeconomic

ABSTRACT

The use of fossil fuels leads to depletion of fuel reserves and environmental pollution. One way to achieve a sustainable future in urban areas and remote communities is to use the independent renewable energy systems. Meanwhile, solar energy is one of the most common sources of energy generation that has attracted of the world. The present study provides the comprehensive examine the performance of two parabolic dish collector and flat-plate collector from energy, exergy, Enviroeconomic and Exergoenviroeconomic view of points. To examine the performance of solar systems, the climatic conditions of two different cities in Asia (Beijing and Tehran) have been used. In addition, the performance of the systems is investigated under different parameters and using different working fluids and MWCNT nanoparticle. It was found that the both solar systems have better overall performance in Tehran than in Beijing. Moreover, in the months when the solar collector has lower exergy efficiency, its use in Tehran compared to that Beijing has a better exergy performance than other months. In addition, the lowest and highest Levelized Cost of Energy are belong to dish collector (in Tehran with water) and flat plate collector (in Beijing with Dowtherm Q), respectively. For Tehran, LCOE of dish collector increases more than 5.5-fold when using water/MWCNT nanofluid instead of water.

1. Introduction

Due to the growth of global industry, anticipations indicative that energy demand in 2040 will be 38% higher than that in 2015. However, this increase in energy consumption leads to a reduction in the conventional fuel sources and an increase in the emission of harmful environmental gases (Aghajani and Ghadimi, 2018). Therefore, to tackle these environmental problems and prevent the depletion of fossil fuel resources, many governments and researchers around the world are looking to use clean and alternative energy sources called renewable energy sources (Huang and Marefati, 2020; Peng et al., 2020). Utilizing these energy sources can reduce greenhouse gases and reduce fossil fuel consumption as well as economic growth (Mehrpooya et al., 2019a; Bagal et al., 2018). The most important sources of renewable energy include wind, solar, geothermal, biomass, etc. (Oyekale et al., 2020). Meanwhile, over the past few decades, energy generation (power and heat) using solar energy systems have grown significantly (Liu et al., 2020; Cai et al., 2019). It is expected that by 2030, the capacity to use solar energy in the EU increase more than ten-fold (Mehrpooya and Marefati, 2020; Ye et al., 2020). Solar energy can be used as separate or hybrid systems as well as in the form of distributed generation (DG) systems, CHP and CCHP systems (Fan et al., 2020; Cheng et al., 2020). Although solar energy systems have very low environmental pollution and can be used in most parts of the world, special systems are needed to convert solar energy (Algieri et al., 2020). There are three major ways to use solar energy: (1) solar photovoltaic (PV) (converting solar energy into electricity) (Li et al., 2020), (2) solar thermal system (converting solar energy into hot water), and (3) CSP technologies (steam production) (Araújo et al., 2019; M. and Ghadimi, 2016). Meanwhile, using solar collectors, solar light energy can be converted into thermal energy by using the working fluid that flows inside the collector (Barbosa et al., 2020). Generally, solar collectors are divided into two models: stationary and concentrated solar collectors. Two examples of

* Corresponding author.
E-mail address: oyp9812@126.com (P. Ouyang).
[1] These authors contribute equally to this paper.

https://doi.org/10.1016/j.egyr.2021.04.046

Nomenclature

A	Area (m^2)
C	Cost ($)
CC_P	Specific heat (J/kg K)
EF	Exergy efficiency (%)
En	Energy rate (W)
Ex	Exergy rate (W)
E1	Environmental parameter
E2	Exergoenvironmental parameter
f	Focal distance (m)
i	Interest rate
G	Solar irradiance (kW/m^2)
k	Thermal conductivity (W/m K)
m	Flow rate (kg/s)
Pr	Prandtl number
QS_g	Thermal power (W)
S_g	Entropy generation (W/K)
T	Temperature (°C)
t	Working hours (h)
y	Operation years

Greek symbol

α_s	Solar angle (°)
ε	Emissivity
η	Efficiency
ρ	Density (kg/m^3)
ϕ	Particle volume fraction

Subscripts

a	Ambient
d	Destruction
F	Base fluid
in	Inlet
nF	Nanofluid
out	Outlet
s	Solar

Abbreviations

CCHP	Combined cooling, heating and power
CSP	Concentrated solar power
DG	Distributed generation
FPC	Flat plate collector
LCOE	Levelized Cost of Energy
PDC	Parabolic dish collector
PV	Photovoltaic
SI	Sustainability index

the collectors are flat plate collector (FPC) and parabolic dish collector (PDC), which operates at temperature of 30–80 °C and 100–1500 °C, respectively (Kalogirou, 2013). The present paper provides a comparative study between the performance of FPC and PDC with various heat transfer fluids from the energy, exergy, and exergoeconomic as well as enviroeconomic points of view. Table 1 presents the differences between the two collectors. One of the major parameters in evaluating concentrating systems is the concentration ratio. The PDC concentration ratio is in the range of 600 to 2000 (Stefanovic et al., 2018). Recently, many scholars have experimentally and theoretically studied the solar collectors' performance with various heat transfer fluids and from different perspectives. The aims of all the studies were to achieve high efficiency and output temperature and low economic costs (Agyekum and Velkin, 2020; Marefati et al., 2018; Sadeghi et al., 2020). Abuşka and Şevik (2017) reported energy and exergy efficiency of 60% and 12% for the FPC system, respectively. They also calculated the payback time for the system for 4.3 years. Diez et al. (2019) modeled the FPC based on an artificial neural method that calculated system output for input data such as solar intensity and temperature. Results revealed that the proposed method can be used for other systems. Bhowmik and Amin (2017) showed a 10% increase in system efficiency for a condition in which the FPC was able to receive both diffuse and beam solar irradiance. Mukherjee et al. (2020) investigated the effect of power and reactive aspect on the operation of the FPC system coupled with the thermochemical energy storage system. They found that, as the power density increases the global reaction advancement rate drops for both discharge and charge modes. The experimental analysis of the FPC system was performed by Khwayyir et al. (2020) in Iraq (Najaf city), considering the air bubble injections influence. They showed a 70% increase in system efficiency for a flow rate of 2 LPM. By examining the FPC performance based on the ASHRAE test standards Tian et al. (2020) concluded that the IAM parameter has a significant influence on the optical performance of the system. Mohamed et al. (2020) examined the experimental performance of FPC system coupled with energy storage system in Egypt. By testing the system performance with different fluid and nanofluid, they showed that the performance of the system improved by 6.8% when using nanofluid. In addition, the average annual capacity of storage system was 4kWh/day. A similar study was performed by Tong et al. (2019) with various nanofluids. The results showed that the exergy and energy performance of the FPC system improved by 57% and 20%, respectively, when Al_2O_3 nanofluid was used. Pavlovic et al. (2018) examined the performance of PDC system by different nanofluids and corrugated and smooth spiral absorber. They concluded that the best performance of the system is achieved when thermal oil is used as the base fluid and copper as the nanoparticle. In a similar study, Loni et al. (2018) an improvement in the thermal and exergetic performance of the system when using water based CuO and Al_2O_3 nanofluids. In that PDC system the concentration ratio was 28.5. In addition, the exergy and energy efficiencies of the system were 10% and 35%, respectively. Yaqi et al. (2011) provided an efficiency of 34% with a concentration ratio of 1300 for the PDC system. Considering the various deign (optical performance, temperature and wind velocity) Stefanovic et al. (2018) provided exergy and energy performance of 22% and 50% for the PDC, respectively. In addition, they found that the best system performance was obtained at flow and temperature of 0.08 l/h and 210°C, respectively. One of the main applications of solar collectors is their use in multi-generation systems. Moradi and Mehrpooya (2017) used PDC to provide 0.6 MW of thermal power for a commercial building (in a CCHP system). The system had a total efficiency of 80%. The PDC was used to supply the domestic hot water at a temperature of 100°C (Mohammed, 2012). Marefati et al. (2019) produced a thermal power of 9.8 MW using a solar collector in a hybrid system. In the system, the solar collector increased the temperature of the fuel cell reformer inlet fluid. In the hybrid system the exergy destruction and exergy efficiency of the solar system were 5.7 MW and 94%, respectively. In another study, they reported the exergy efficiency of 48% for the solar system coupled with fuel cell and thermoelectric generator (Marefati and Mehrpooya, 2019). Shariatzadeh et al. (2015) examined the operation of the electrolyzer, fuel cell and solar thermal hybrid system. The system is able to produce 300 g/s of hydrogen fuel at peak solar irradiation. Gavagnin et al. (2017) studded the economic performance

Table 1
Comparison between the two FPC and PDC systems.

Collector	Specification
FPC	Operating temperature range: 30–80 °C Type of absorber : Flat Tracking: Stationary Concentration ratio: 1 Efficiency: Low Relative cost: Low Technology maturity: Very mature
PDC	Operating temperature range: 150–2000 °C Type of absorber: Point Tracking: Two-axis Concentration ratio: 600–2000 Efficiency: High Relative cost: Very high Technology maturity: Recent

of the dish collector coupled gas turbine based on equipment manufacturers data. The cost of implementing the system was 5.61 $/W. Mohammadi and Mehrpooya (2018) reported the efficiency of 73% for electrolyzer and dish collector hybrid system to produce hydrogen fuel. By experimental study and using the data obtained in numerical modeling, Pavlovic et al. (2017) found that the system with spiral type absorber and in the use of water and thermal oil had the best performance. In addition, the highest exergy performance was related to 155 °C (if using oil). In another application, Hafez et al. (2016) provided the heat required by the Stirling engine from the thermal power generated by the PDC. The optimization of system was examined to determine the degree of deviation from the ideal state (Ahmadi et al., 2013).

The use of conventional fuels has two major problems: depletion of reserves and air pollution. The future of energy demands for human society is related to renewable energy. Meanwhile, solar energy is one of the most common renewable sources of electricity and heat generation that has attracted of the world. However, the operation of solar energy systems is associated with some challenges and obstacles. The aim of this paper is to investigate and comparison two stationary and concentrating solar collectors from energy and exergy points of view. In the present work, the performance of two FPC and PDC solar collectors in Tehran and Beijing are investigated. The influence of using various fluids and nanofluids as a HTF on performance solar thermal systems is examined. The use of nanofluids as a new medium for heat transfer can have a significant effect on increasing the rate of heat transfer, consequently leading to improved solar collectors performance. A review of the literature revealed that such a comprehensive study on stationary and concentrating solar collectors that examine climate data for two different cities in Asia has not been studied. In addition, parameters such as LCOE, Enviroeconomic (E_1) and Exergoenviroeconomic (E_2), entropy generation rate and Sustainability index for solar systems are investigated and compared. Moreover, the results provided in the present paper do not correspond to any of the findings of previous similar studies. Therefore, the main objectives of this work are to comprehensively study the performance of two types of solar collectors for thermal energy generation and compare them in Tehran and Beijing, decreasing the consumption of fossil fuel, consequently decreases the pollutants emissions by use of clean energy and ability to apply the obtained results for use in experimental works. Furthermore, the obstacles and challenges of solar energy development in Iran and China are discussed. Overall, the obtained results of research and challenges raised are very encouraging and useful for governments and energy systems engineers and designers.

The rest sections of this paper are as follows: Section 2 describes the numerical modeling of the two solar collectors, LCOE, Enviroeconomic and exergoenviroeconomic parameters and heat transfer fluids specifications. Section 3 provided the climatic data. Section 4 presents the simulation results and carries out the analysis of performance assessment parameters; Section 5 summarizes the conclusion of this paper.

2. Numerical modeling

In present paper, in order to examine the performance of FPC and PDC systems, the energy, exergy, enviroeconomic and exergoeconomic assessments are performed. Herein, the explanations and important relationships related to the mathematical modeling of solar systems are provided. It should be noted that, numerical modeling data from the available literature are chosen. Fig. 1 presents the solar collectors control volume.

2.1. Flat plate solar collector

FPC is one of the most common stationary collectors that operates at low temperatures and is mostly used to provide hot water for buildings. This collector has a simple design, easy maintenance and low operating costs. It also has the ability to receive both beam and diffuse solar radiation. FPCs must be oriented south in the northern hemisphere (Tanaka, 2015). In steady state conditions the FPC and PDC energy balance is written as (Caliskan, 2017):

$$En_{F,i} - En_{F,o} = En_{loss} - En_{S,i}$$
$$\text{where, } \begin{cases} En_{F,i} \text{ and } En_{F,o}: \text{Input and output energy of working fluid} \\ En_{loss}: \text{Loss energy of system} \\ En_{S,i}: \text{Input energy of solar} \end{cases} \quad (1)$$

Furthermore, the fluid net energy is determined as (Chen et al., 2012):

$$\Delta En_F = En_{F,o} - En_{F,i} = m_F \times C_{P,F} \times (T_o - T_i)$$
$$\text{where, } \begin{cases} C_{P,F}: \text{Specific heat of fluid} \\ m_F: \text{Mass flow rate of fluid} \\ T_i: \text{Fluid inlet temperature of solar collector} \\ T_o: \text{Fluid outlet temperature of solar collector} \end{cases} \quad (2)$$

The solar collectors' exergy balance can be determined by Eq. (3) (Huang and Marefati, 2020):

$$Ex_{F,i} - Ex_{F,o} = Ex_{loss} + Ex_d - Ex_{S,i}$$
$$\text{where, } \begin{cases} Ex_{F,i} \text{ and} Ex_{F,o}: \text{Input and output exergy of working fluid} \\ Ex_{loss}: \text{Loss exergy of system} \\ Ex_d: \text{Exergy destruction of system} \\ Ex_{S,i}: \text{Input exergy of solar} \end{cases} \quad (3)$$

The fluid net exergy is determined as (Chen et al., 2012):

$$\Delta Ex_F = Ex_{F,o} - Ex_{F,i} = m_F \times C_{P,F} \times \left[\left[(T_o - T_a) - T_a \times \ln\left(\frac{T_o}{T_a}\right) \right] - \left[(T_i - T_a) - T_a \times \ln\left(\frac{T_i}{T_a}\right) \right] \right] \quad (4)$$

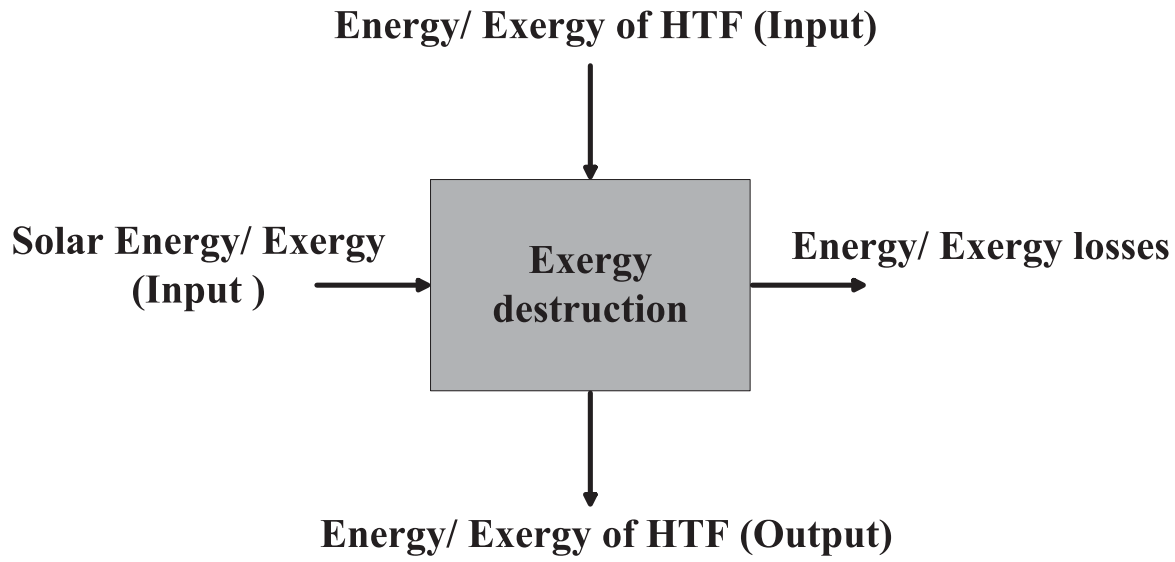

Fig. 1. Solar thermal collectors control volume.

The input $En_{s,i}$ and $Ex_{s,i}$ can be obtained by the following relations (Barreto and Canhoto, 2017):

$$\begin{cases} En_{S,i} = G \times A_{coll} \\ Ex_{S,i} = En_{S,i} \times \left[1 + \frac{1}{3} \times (\frac{T_a}{T_s})^4 - \frac{4}{3} \times (\frac{T_a}{T_s})\right] \\ G: \text{Solar irradiance} \\ A_{coll}: \text{Aperture area of solar collector} \\ T_a: \text{Ambient temperature} \\ T_s: \text{Sun temperature} \end{cases} \quad (5)$$

Moreover, Eqs. (6) and (7) can be used to determine the loss energy and exergy of the FPC (Deng et al., 2016):

$$En_{loss} = Q_{rad} + Q_{conv}$$

$$\text{where, } \begin{cases} Q_{rad} = \varepsilon \times \sigma \times A_{coll} \times (T_{surf}^4 - T_a^4) \\ Q_{conv} = h \times A_{coll} \times (T_{surf} - T_a) \\ h: \text{Coefficient of convection heat transfer} \\ \quad \rightarrow h = \dfrac{0.15 \times Ra^{0.33} \times k}{L} \\ Ra: \text{Rayleigh number} \rightarrow Ra \\ = \dfrac{g \times Cos(\theta) \times L^3 \times \Pr \times (T_{surf} - T_{\ a})}{\upsilon^2} \\ \Pr: \text{Prandtl number} \\ L: \text{System characteristic length} \end{cases} \quad (6)$$

and,

$$Ex_{loss} = Ex_{rad} + Ex_{conv}$$

$$\text{where, } \begin{cases} Ex_{rad} = Q_{rad} \times (1 - \dfrac{T_a}{T_{surf}}) \\ Ex_{conv} = Q_{conv} \times (1 - \dfrac{T_a}{T_{surf}}) \end{cases} \quad (7)$$

Using the following equations, the energy and exergy efficiencies of the FPC can be calculated (Caliskan, 2015):

$$\begin{aligned} &\text{Energy efficiency} \rightarrow \eta_{En,FPC} = \frac{\Delta En_F}{En_{S,i}} \\ &\text{Exergy efficiency} \rightarrow \eta_{Ex,FPC} = \frac{\Delta Ex_F}{Ex_{S,i}} \end{aligned} \quad (8)$$

2.2. Parabolic dish solar collector

PDC systems are made of a dish mirror array to reflect and concentrate incoming sunlight onto a collector to provide enough heat to efficiently convert heat into energy. This requires the dish to track the sun along two axes. The concentrated sunlight is absorbed by the receiver and transmitted to an engine (Cherif et al., 2019; Mehrpooya et al., 2019b). PDCs are classified as technologies with high efficiency, modularity, independent operation, and intrinsic hybridization (operation based on solar energy and fossil fuels or both). Among all solar systems, PDCs have the best solar-to-electricity performance and thus have the highest potential to become the cheapest source of renewable energy (Charalambous et al., 2011). The modularity of these technologies allows them to be deployed independently for remote applications and small grids (rural electricity). However, the system is in the stage of engineering development, and there are still technical challenges with solar components and the ability to commercialize an engine exclusively for solar applications (Huang and Marefati, 2020). In concentrating solar collectors, in addition to thermal performance, optical analysis should also be considered. The optical performance of the concentrating solar collector has a key role in the amount of solar absorbed by the collector. Important parameters for evaluating the optical performance of a PDC are concentration ratio, receiver diameter, focal length and distance between focal point and receiver (Beltrán-Chacon et al., 2015). To calculate the concentration ratio of PDC, the following steps must be performed (Mehrpooya and Marefati, 2020):

(1) Calculate the focal length

$$f = \frac{0.25 \times D_c}{\tan(\frac{\phi_r}{2})} \quad (9)$$

where, ϕ_r and Dc represent the rim angle and dish diameter, respectively.

(2) Calculate the lateral distance between the focus point of receiver and concentrator surface

$$P = \frac{2f}{1 + \cos(\varphi)} \quad (10)$$

(3) Calculate the beam spread

$$\Delta_b = \tan(\frac{\sigma \times n}{2}) \times 2 \times P \quad (11)$$

where, σ is the total optical error.

(4) Calculate the diameter of receiver

$$D_r = \frac{\Delta_b}{\cos(\phi_r)} \tag{12}$$

(5) Calculate the distance between the focus point and receiver

$$d_f = \frac{D_r \times \left(f - \frac{D_c^2}{16f}\right)}{D_c} \tag{13}$$

(6) Calculate the optimal height of receiver

$$H = f - d_f \tag{14}$$

(7) Calculate the concentration ratio

$$C = \left(\frac{\cos\left(\phi_r + \frac{\alpha_s+\delta_d}{2}\right) \times \sin(\phi_r)}{\sin\left(\frac{\alpha_s+\delta_d}{2}\right)}\right)^2 \tag{15}$$

where, α_s and $\delta_d$are the solar and dispersion angles, respectively. To examine the thermal performance of the PDC, its output power and energy efficiency should be determined as follows (Hafez et al., 2016):

$$Q_{PDC} = Q_s - Q_{loss}$$
$$where, \begin{cases} Q_s = C \times G_b \times \rho \times A_{coll} \\ Q_{loss} = Q_{cond} + Q_{conv} + Q_{rad} \end{cases} \tag{16}$$

Table 2 provides the relationships required to calculate PDC losses. Furthermore, the next equation is used to determine the PDC energy efficiency (Yaqi et al., 2011):

$$\eta_{En-PDC} = \frac{Q_{PDC}}{Q_s} \tag{17}$$

Eventually, Eq. (18) can be used to determine the exergy efficiency of PDC (Petela, 2003):

$$\eta_{Ex,PDC} = \frac{Ex_u}{Ex_s}$$
$$\text{where, } \begin{cases} Ex_s = Q_s \times \left(1 - \frac{4}{3} \times (\frac{T_a}{T_s}) + \frac{1}{3} \times (\frac{T_a}{T_s})^4\right) \\ Ex_u = Q_{PDC} - \left(m_F \times C_{P,F} \times T_a \times \ln(\frac{T_o}{T_i})\right) \end{cases} \tag{18}$$

Two main indexes in the exergy performance of a system are sustainability index (SI) and the entropy generation rate (S_g). Sustainability index presents how enhancement of the exergy efficiency of a solar system can reduce its environmental effects. Sustainability index and the entropy generation rate are related to exergy efficiency and exergy destruction, respectively, and are obtained by the following equations (Fudholi et al., 2019):

$$SI = \frac{1}{1 - \eta_{Ex}} \tag{19}$$

$$S_g = \frac{Ex_d}{T_a} \tag{20}$$

Based on the above equations, it can be said that these two parameters change with exergy values.

2.3. Levelized cost of energy

Levelized cost of energy (LCOE) is a parameter that provides the minimum price of electricity generated by the energy system in $/kWh. This parameter indicates the economic viability of the solar system and is determined as follows (Boukelia et al., 2016; Hamian et al., 2018):

$$LCOE = \frac{C_{investment} + C_{O\&M}}{Q_{coll} \times t} \times \frac{i \times (1+i)^y}{(1+i)^y - 1}$$
$$\text{where, } \begin{cases} i: \text{Interest rate} \rightarrow \text{i} = 8\% \\ y: \text{OperationYears} \rightarrow \text{y} = 20 \text{ years} \\ t: \text{Working hours} \rightarrow \text{t} = 6\text{h}/day \end{cases} \tag{21}$$

where, i, y and t represent the interest rate, operation years and working hours, respectively. The values of i, y and t were selected to 8%, 20 years and 6 h per day, respectively. Note that in the present study, the solar system purchase includes only FPC/ PDC, HTF, maintenance costs, and other ancillary costs are excluded.

2.4. Enviroeconomic and exergoenviroeconomic parameters

One of the important aims of the solar systems development is to decrease the emission of environmental pollutants. Life-cycle assessment (LCA) balances materials and energy throughout the life of a solar collector (Yu et al., 2020). In this index, research objectives and boundaries should be considered for accurate evaluation of the system. LCA is presented in four separate stages (definition of scope and goal, inventory analysis, impact evaluation and interpretation), the various stages often being interrelated in that the results of one stage can determine how the other stages are completed. By calculating the LCA, its impact on the environment can be determined. By determining the amount of energy output and CO_2 produced by the solar system in operating time, its environmental effects can be assessed. In this paper, for the environmental analysis of solar thermal systems, the LCA and carbon pricing methods (enviroeconomic aspect, to reduce or cut the CO_2 emission) are used. So, the enviroeconomic assessment is provided as a tool to evaluate the solar collectors' carbon pricing. In addition, by considering the three parameters of exergy rate, value of CO_2 emission (based on LCA), and hours of working, an exergoenvironmental assessment (information about exergy performance based on carbon dioxide value) can be provided. The difference between exergoenvironmental analysis and environmental analysis is in their data. In environmental analysis, energy results are used and in exergoenvironmental analysis, exergy results are used. Finally, to assess the amount of CO_2 emission, another analysis called an exergoenviroeconomic analysis can be used. The determination of this index, in addition to the first law, is important in terms of the first and second thermodynamics laws. The following equations can be used for enviroeconomic (E_1) and exergoenviroeconomic (E_2) assessments of solar collector (Caliskan et al., 2012):

$$E_1 = x_{CO_2} \times En_{s,i} \times t \times C_{CO_2}$$
$$\text{where, } \begin{cases} C_{CO_2}: CO_2 \text{ emission price} \\ x_{CO_2}: \text{Value of } CO_2 \end{cases} \tag{22}$$

and,

$$E_2 = x_{CO_2} \times Ex_{s,i} \times t \times C_{CO_2} \tag{23}$$

2.5. Heat transfer fluids

In this study, two types of heat transfer fluids, namely water and Dowtherm Q, are used to investigate the solar systems performance. In addition, the impact of the use of nanofluids on the performance of systems is investigated. Dowtherm Q is a synthetic organic HTF containing a mixture of alkylated aromatics and diphenylethane. Compared to hot oils, it represents better thermal consistency and significantly better low-temperature pump ability. Moreover, the nanoparticle examined in this work

Table 2
The relationships required to calculate PDC losses Mehrpooya and Marefati (2020).

Parameter	Description	Equation
Q_{cond}	Conduction loss	Neglected in this paper
Q_{rad}	Radiation loss	$Q_{rad} = (T_w^4 - T_a^4) \times A_c \times \sigma \times \varepsilon_{eff}$ T_w: Temperature of cavity wall A_c: Receiver area $\varepsilon_{eff} = \frac{1}{1+(\frac{1}{\varepsilon_c}-1)\times\frac{A_c}{A_w}}$; $\begin{cases} A_w/A_c > 5 \\ 0.8 < \varepsilon_c < 1 \end{cases}$
Q_{conv}	Convection loss	$Q_{conv} = (T_w - T_a) \times A_w \times h_c$
$h_c = \frac{0.0196 \times Ra_L^{0.41} \times \mathrm{Pr}^{0.13} \times K}{\left\lvert \sum_{i=1}^{3} a_i \cos(\phi + \theta_i)^{b_i} \times L_i \right\rvert}$		
$Ra_L = \frac{\left\lvert \sum_{i=1}^{3} a_i \cos(\phi + \theta_i)^{b_i} \times L_i \right\rvert^3 \times g \times \beta \times (T_w - T_a)}{\alpha \times \upsilon}$		
$\mathrm{Pr} = \upsilon/\alpha$		

is multi-walled carbon nanotubes (MWCNT). MWCNT has extraordinary thermal properties and can be widely used industrially and commercially as a new generation of refrigerants and thermal operating fluids. The use of these nanofluids in thermal systems can increase the efficiency and significantly increase the Nusselt number and heat transfer coefficient in equal Reynolds. This group of nanofluids in different base fluids such as ethylene glycol and water with suitable stability can be provided. The physical properties of the nanofluid should be determined based on the nanoparticle and base fluid physical properties. These properties include viscosity, density, thermal conductivity and specific heat Ehyaei et al. (2019). The physical properties of nanofluids can be obtained using the following equations (Khanjari et al., 2016; Loni et al., 2017; Zadeh et al., 2015):

$$\begin{cases} \text{Density} \rightarrow \rho_{nF} = \rho_F \times (1-\varphi) + (\rho_{nP} \times \varphi) \\ \text{Viscosity} \rightarrow \mu_{nF} = \mu_F \times \left(1 + 2.5 \times \varphi + 6.5 \times \varphi^2\right) \\ \text{Specific heat} \rightarrow C_{P,nF} = C_{P,F} \times \dfrac{\rho_F \times (1-\varphi)}{\rho_{nF}} \\ \quad + C_{P,nP} \times \dfrac{\rho_{nF} \times \varphi}{\rho_{nF}} \\ \text{Thermal conductivity} \rightarrow k_{nF} \\ = k_F \times \dfrac{k_{nP} + (2 \times k_F) + \left[2 \times \varphi \times (k_{nP} - k_F) \times (1+\beta)^3\right]}{k_{nP} + (2 \times k_F) - \left[\varphi \times (k_{nP} - k_F) \times (1+\beta)^3\right]} \end{cases} \quad (24)$$

The required data for mathematical modeling are given in Table 3. In addition, the following assumptions are considered to examine the solar systems performance:

- The FPC and the PDC have the same aperture area;
- FPC and PDC can work with a variety of heat transfer fluids as well as in the considered climate;
- The end losses, shadow effects and other effects on collector performance are ignored.

3. Climatic data

Due to the different latitudes, climatic conditions and altitude, the amount of solar energy received in any region is different. Two important climatic parameters in the performance of solar systems are the solar irradiance and ambient temperature. In this work, to examine the performance of the FPC and PDC systems the climatic conditions of Beijing (in China) and Tehran (in Iran) are considered. The geographical characteristics of Beijing and Tehran are 39.5°N, 116.2°E and 35.7°N, 51.4°E, respectively. According to Fig. 2, the average solar irradiance in Beijing and Tehran is 0.28 and 0.46kW/m^2, respectively. Moreover, average ambient temperature in Beijing and Tehran are 12.86, 18.39 °C, respectively (see Fig. 3).

Table 3
The required data for numerical modeling of solar collectors.

Parameter	Rate	Parameter	Rate
A_{coll}	8.3 m^2	C_{CO2}	0.0146$/kg
$T_{i,FPC}$	40 °C	ρ	0.94
$T_{i,PDC}$	120 °C	i	8%
m_F	0.03 kg/s	y	20 years
t	6 h/d	φ	3%
T_S	6000 K	ρ_{MWCNT}	2100 kg/m^3
α	0.88	k_{MWCNT}	3000 W/m K
C_{PDC}	1850	$C_{P,MWCNT}$	796 J/kg K
ε	0.9		

4. Result and discussion

Section 4 first compares the results of solar collectors mathematical modeling with the literature data which are done by Caliskan (2017) and Karimi et al. (2019). The comparisons results are presented in Table 4 for FPC and PDC systems. It should be noted that the design data mentioned in the references are used to validate. The highest deviation in energy efficiency and outlet temperature of solar collector is 1.48% and 0.9%, respectively. These errors are relatively low and therefore the numerical modeling performed in the present study can be considered reasonable and reliable. The results obtained for the FPC and PDC in Tehran and Beijing are discussed.

4.1. Energy performance

Determining the useful output power of a solar collector is one of the essential parameters in evaluating its performance. In general, more intensity of solar radiation leads to more output of the solar system. In the previous section, it was mentioned that

Table 4
Numerical model validation results.

G (W/m^2)	T_i (°C)	Literature		This paper			
		T_o (K)	η_{En}(%)	T_o (K)	Deviation	η_{En}(%)	Deviation
FPC Caliskan (2017)							
650	25	31.25	25.3	31.05	0.64%	24.93	1.48%
PDC Karimi et al. (2019)							
1000	62	89.9	52.81	89.1	0.9%	52.32	0.93%

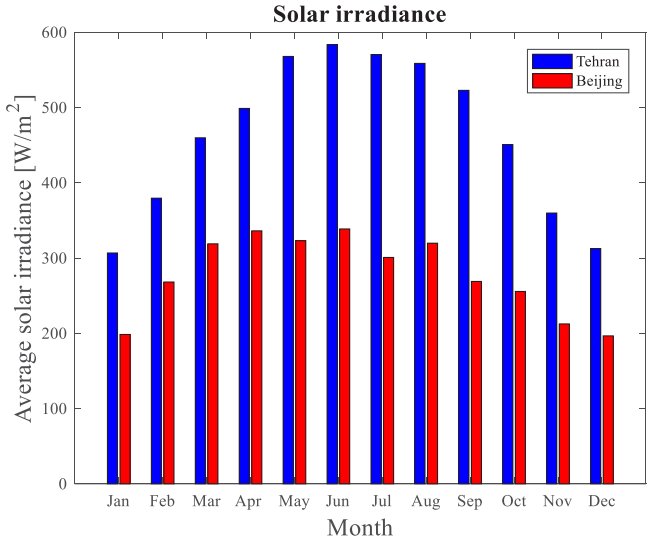

Fig. 2. Monthly average solar irradiance in selected regions (Meteotest, 2000).

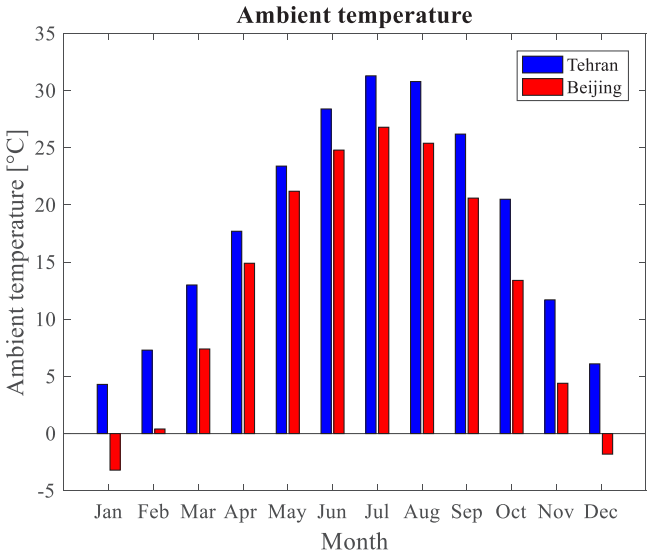

Fig. 3. Monthly average ambient temperature in selected regions (Meteotest, 2000).

the monthly average solar irradiance in Tehran is 66.93% higher than that in Beijing. Therefore, it is expected that the useful output power of solar collectors in Tehran will be higher than that in Beijing. The monthly average useful power output of PDC and FPC in Beijing and Tehran is illustrated in Fig. 4. The average useful output power of the PDC in Beijing is 94.7% lower than that in Tehran. In addition, in both regions, the highest useful power output of the PDC is related to the Jun. However, the useful output power of the collector in Jun for Tehran is 95.2% higher than that in Beijing. Also, the lowest useful output power of the PDC system is obtained in Tehran and Beijing at Jan and Dec, respectively. The lowest PDC useful output power in Tehran is 95.84% more than that in Beijing. In addition to the solar insolation, according to the radiation loss relationship in Table 2, it is clear that with increasing ambient temperature, the amount of radiation loss of PDC decreases. Since the average ambient temperature in Tehran is 5.53 degree higher than that in Beijing, the radiation loss of the PDC system in Beijing are higher than that in Tehran, which leads to a decrease in the collector output power in Beijing. The same trend is shown for FPC system. With the difference that the average useful output power of the FPC in Tehran is 48.14% higher than that in Beijing. Similarly, the highest and lowest useful output power of the FPC in Tehran (Beijing) is related to Jun (Jun) and Jan (Dec), respectively. It was also found that, due to the low average ambient temperature in Beijing compared to Tehran, the FPC has more losses in Beijing than Tehran, which leads to lower useful output power of FPC in Beijing than in Tehran. In addition, it was apparent that assuming the similar conditions; PDC produces 146.1% and 87.2% high useful power than the FPC in Tehran and Beijing, respectively. The main reason for this more power produced by PDC is due to the inherent nature of concentrating solar collectors. In concentrating solar collectors, due to the use of the solar tracking system, the sunlight receives more intense radiation, which leads to the production of more energy.

The next parameter in evaluating the energy performance of the solar collector is energy efficiency. Fig. 5 shows the monthly average energy efficiency of PDC and FPC in selected regions. According to Eqs. (8) and (17), by increasing the Q of the solar collector, its energy efficiency increases. The average PDC energy efficiency in Beijing is 17.21% lower than that in Tehran. In addition, in both regions, the highest energy efficiency of the PDC is related to the Jun. However, the collector energy efficiency in Jun for Beijing is 13.31% lower than that in Tehran. Also, the lowest energy efficiency of the PDC system is obtained in Tehran and Beijing at Jan and Dec, respectively. The lowest PDC energy efficiency in Tehran is 25.48% more than that in Beijing. Similar to PDC, the FPC system in Tehran has a higher energy efficiency compared to Beijing. The average FPC energy efficiency in Beijing is 30.06% lower than that in Tehran. In addition, the highest energy efficiency obtained from the FPC in Tehran is 20.6% higher than that in Beijing. However, the FPC system in Beijing has very low energy efficiency in the colder months of the year (i.e., Jan and Dec). For instance, the energy efficiency of FPC (in Jan) in Beijing is about 3-fold lower than that in Tehran. This is because the solar radiation and ambient temperature in Tehran (at the Jan) is about 54.5% and 7.5 degree, respectively, higher than that in Beijing. Furthermore, it was found that assuming the similar conditions; the average energy efficiency of PDC is 45.45%

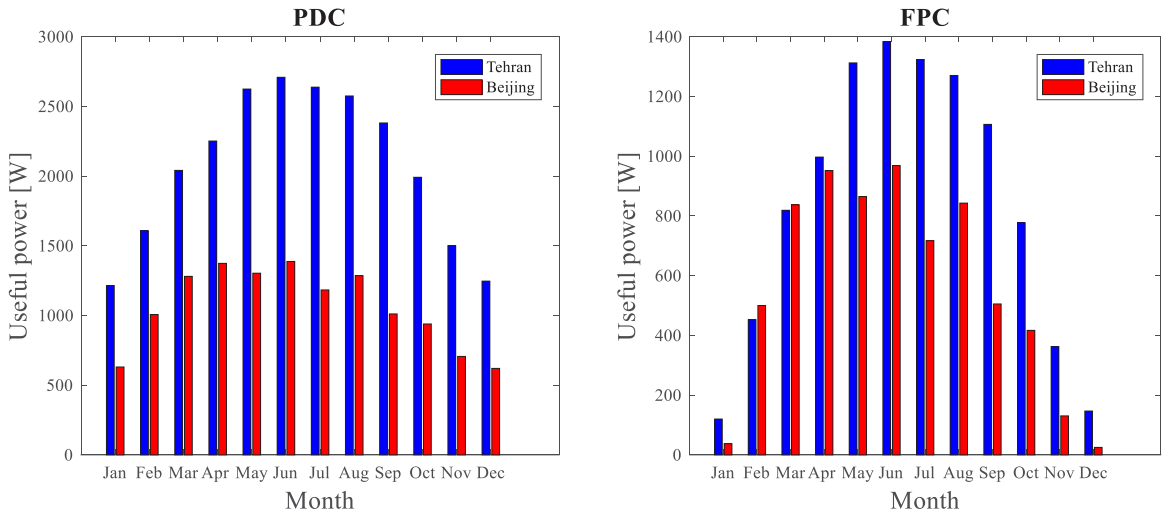

Fig. 4. Monthly average useful power output of PDC (left) and FPC (right) in selected regions.

and 61.4% higher than that of the FPC in Tehran and Beijing, respectively. Therefore, it can be said that, in both regions, the PDC has better energy performance compared to the FPC. In other words, to provide the certain thermal energy, a smaller area of the PDC is required compared to the FPC. However, the cost of the PDC is higher than the FPC that should be considered.

Another main factor in evaluating the solar collectors operation is the temperature of its outlet heat transfer fluid. Note that in this paper, the temperature of the inlet fluid in the PDC and FPC is 120 and 40 °C, respectively. Therefore, in order to rationally investigate the difference between the outlet and inlet temperature of the heat transfer fluid was calculated. The monthly average increased temperature (or temperature difference; TD) of the outlet fluid in PDC and FPC in selected regions is demonstrated in Fig. 6. Obviously, the PDC generates more thermal energy with higher temperatures. The average temperature difference of the PDC in Tehran is 8.01 degree higher than that in Beijing. Furthermore, in both regions, the highest increased temperature of the PDC is related to the Jun. However, the TD of the collector in Jun for Tehran is 10.53 degree higher than that in Beijing. Also, the lowest temperature difference of the PDC system is obtained in Tehran and Beijing at Jan and Dec, respectively. The lowest temperature difference of PDC in Tehran is 4.74 degree more than that in Beijing. Similar to PDC, the FPC system in Tehran has a higher increased temperature compared to in Beijing. The average TD of the FPC in Beijing is 2.18 degree lower than that in Tehran. In addition, the highest temperature difference obtained from the FPC in Tehran is 3.31 degree higher than that in Beijing. However, the FPC system in Beijing has very low TD in the colder months of the year (i.e., Jan and Dec). For instance, the increased temperature of FPC (in Jan) in Beijing is about 3.2-fold lower than that in Tehran. This is because the solar radiation and ambient temperature in Beijing (at the Jan) is lower than that in Tehran. Furthermore, it was found that assuming the average TD of PDC is 9.77 and 3.94 degree higher than that of the FPC in Tehran and Beijing, respectively. Therefore, in both cities, the PDC generates warmer thermal energy.

4.2. Exergy performance

Irreversibility in practical processes produces entropy and exergy destruction. To investigate the exergy operation of the FPC and PDC systems, the exergy destruction (ED) and exergy efficiency (EF) should be calculated. By investigation the exergy performance, a better view can be obtained for the design of the system. The unavoidable ED is a main part of solar system ED. Based on relationships described in Section 2, the exergy operation of FPC and PDC depends on net exergy of heat transfer fluid, exergy losses, exergy destruction and input exergy of solar collector. However, the net exergy of heat transfer fluid depends on specific heat, flow rate and inlet and outlet temperatures of fluid as well as ambient temperature. In addition, the input exergy of solar collector depends on input energy and T_a and T_s. Since the input energy of the solar system depends on the solar irradiance, so the exergy performance of the system also depends on the solar radiation (see Eq. (5)). Therefore, the use of FPC and PDC collectors in each region with different climatic conditions will have different exergy operation. The monthly average EF and ED of PDC and FPC systems in Tehran and Beijing are illustrated in Figs. 7 and 8, respectively. The PDC thermal energy production in Tehran and Beijing has a superior exergy performance than FPC, where the average exergy efficiency of the PDC is more than 5-fold higher than that FPC in Tehran and Beijing. Furthermore, the average EF of the PDC in Beijing is 14.87% lower than that in Tehran. However, this value is 11.47% for the FPC. In both regions, the highest EF of the PDC is related to the Mar. However, the EF of the PDC in Mar for Tehran is 7.41% higher than that in Beijing. Moreover, the lowest EF of the PDC is obtained in Tehran and Beijing at Aug and Jul, respectively. The lowest PDC exergy efficiency in Beijing is 17.36% lower than that in Tehran. Therefore, it can be said that, in the months when the solar collector has lower exergy efficiency, its use in Tehran compared to that Beijing has a better exergy performance than other months. It was found that the highest EF of the FPC in Beijing is 20.35% higher than that in Tehran. However, the lowest EF of FPC in Tehran is about 4-fold higher than in Beijing. So, it lead to the average EF of FPC in Beijing is lower than in Tehran. For instance, the EF of FPC (in Jan) in Beijing is about 2.5-fold lower than that in Tehran.

Meanwhile, solar collectors have more exergy destruction in Tehran than in Beijing. It was found that, the average ED of the PDC in Beijing is 61.95% lower than that in Tehran. This value is significantly less for the FPC and is equal to 17.18%. In both cities, the highest exergy destruction of PDC and FPC is related to Jul and Jun, respectively, which in Tehran is 35.75% and 19.76% more than in Beijing. In addition, the lowest ED of FPC in Beijing is 9.92% and 19.76% lower than in Tehran. However, the lowest exergy destruction of PDC (in Jan) in Tehran is significantly higher (more than 20-fold) compared to in Beijing (in Dec). Meanwhile, the exergy efficiency of PDC in Jan and Dec in Tehran is 19% and 20.3% higher than in Beijing, respectively. Therefore, it can

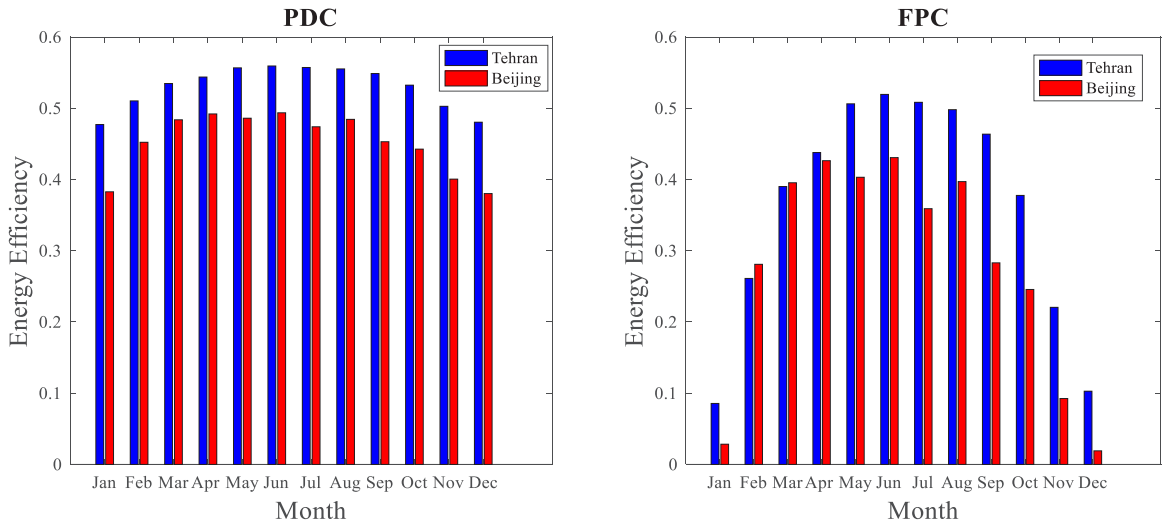

Fig. 5. Monthly average energy efficiency of PDC (left) and FPC (right) in selected regions.

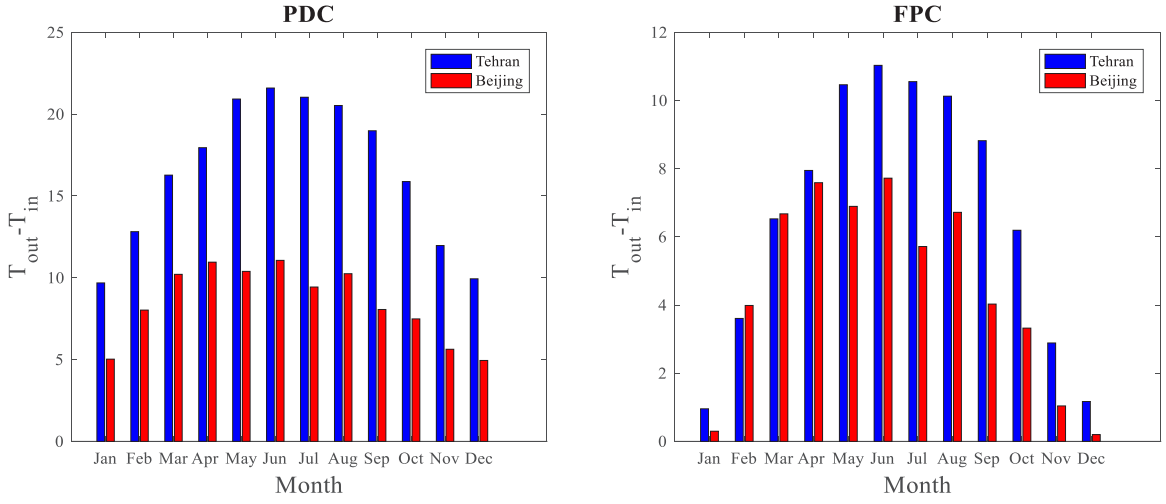

Fig. 6. Monthly average increased temperature of the outlet fluid in PDC (left) and FPC (right) in selected regions.

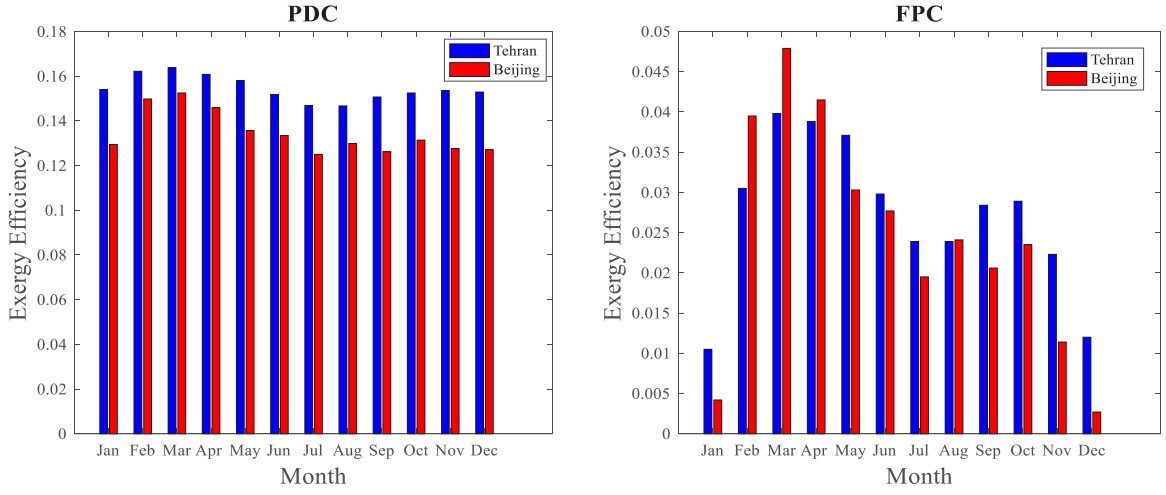

Fig. 7. Monthly average exergy efficiency of PDC (left) and FPC (right) in selected regions.

be said that in throughout the year, the PDC in Tehran has significant exergy performance than in Beijing. In general, more ED means the system has low exergy losses and by rising the input exergy of solar collector (increasing solar radiation), the ED of the system increased. Therefore, the exergy performance of both solar collectors in Tehran is better than in Beijing (due to

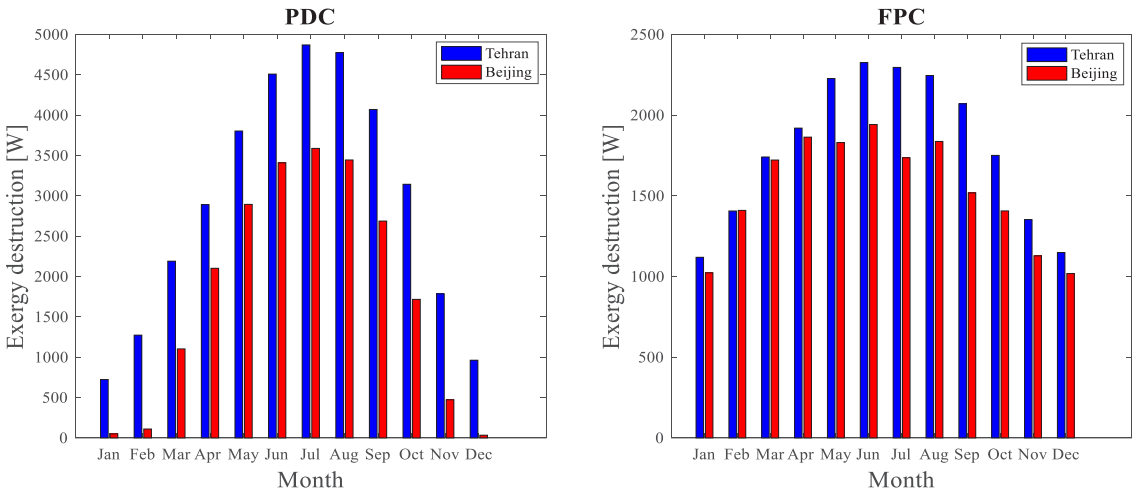

Fig. 8. Monthly average exergy destruction in PDC (left) and FPC (right) in selected regions.

the high average solar radiation in Tehran compared to Beijing). In addition, it was found that in similar design conditions the PDC has superior exergy and energy performances than the FPC.

As mentioned, two main indexes in the exergy investigation of the solar collectors are the SI and the S_g. Sustainability index and the entropy generation rate are related to EF and ED, respectively. Using S_g parameter, the effect of irreversibility in the solar system can be measured. The value of this parameter depends on the nature of the process. In general, S_g can be achieved by subtracting the entropy change from entropy transfer. According to Eq. (20), the value of S_g is directly related to ED and increases with decreasing ambient temperature. Since both the PDC and FPC had higher exergy destruction in Tehran than in Beijing, solar systems generate more entropy in Tehran. Fig. 9 illustrated the monthly average value of S_g for PDC and FPC in selected regions. The average S_g for the PDC in Beijing is 60.94% lower than that in Tehran. In addition, in both regions, the highest value of S_g of the PDC is related to the Jul. However, the value of S_g of the collector in Jul for Beijing is 33.7% lower than that in Tehran. Also, the lowest value of S_g of the PDC system is obtained in Beijing and Tehran at Dec and Jan, respectively. However, the lowest PDC entropy generation rate in Tehran (2.6 W/K) is significantly higher compared to in Beijing (0.12 W/K). The same trend is found for FPC system. The average value of S_g of the FPC in Beijing is 14.79% lower than that in Tehran. But in the FPC system the highest value of S_g of the FPC in Beijing and Tehran is related to Jun. It was also found that, the average ED of PDC in Tehran is 61.95% higher than in Beijing. However, the average value of S_g of PDC in Beijing is 60.94% lower than in Tehran. The reason is that the average ambient temperature in Tehran is higher than in Beijing. In addition, the PDC generates 60.7% and 14.6% more entropy in Tehran and Beijing, respectively, compared to the FPC. Therefore, it is concluded that the PDC system in Tehran have more potential to generate entropy.

On the other hand, according to Eq. (19), the system that has better exergy performance has a higher sustainability index. A high sustainability index means a reduction in the environmental impact of the energy system. Since both the PDC and FPC had higher exergy efficiency in Tehran than in Beijing, solar systems will have higher SI in Tehran. Fig. 10 demonstrated the monthly average SI rate of PDC and FPC in Tehran and Beijing. The average SI rate of PDC in Tehran and Beijing is 15.06% and 12.71% higher than the value in the FPC system, respectively. This means that the PDC has more positive effects on the environment than the FPC system; because under the same conditions, the PDC converts more solar energy into thermal energy (due to its concentrating nature).

4.3. Different heat transfer fluids

In this subsection, the FPC and PDC performances with various HTFs is investigated. These heat transfer fluids include water, Dowtherm Q, and water/MWCNT and Dowtherm Q/MWCNT nanofluids. Fig. 11 shows the SEM image and XRD graph of MWCNT particles. The diameter of MWCNT is between 20 nm and 50 nm. It has been shown that the performance of a solar collector can be significantly improved by adding amounts of nanoparticles to the working fluid. The benefit of nanofluids as a working fluid raises the thermal conductivity, which leads to more thermal energy production. In other words, by increasing the thermal conductivity, more thermal energy is produced at higher temperatures. That is, the difference between the inlet and outlet temperatures of the solar collector increases. Fig. 12 shows the thermal conductivity of different HTFs versus particle volume fraction. Obviously, by adding nanoparticle to the working fluids, the value of k of the heat transfer fluid increases. For instance, at $\phi = 5\%$, the value of k of water/MWCNT nanofluid is 21.36% higher than that of water. In such a context, the thermal conductivity of the Dowtherm Q/MWCNT nanofluid is 21.42% higher than that of Dowtherm Q. Water heat capacity is higher than Dowtherm Q, so PDC and FPC systems are expected to have better energy and exergy performance when using water. Table 5 presents the temperature difference (in degree) of PDC and FPC with different heat transfer fluids in Tehran and Beijing. Using Dowtherm Q instead of water as the working fluid of solar collectors decreases their outlet temperature. The average temperature difference of the PDC and FPC in Tehran when using Dowtherm Q are decreased by 7.84 and 3.19 degrees, respectively. These values in Beijing are 4.02 and 2.15 degrees for PDC and FPC, respectively. However, using nanofluids instead of base fluids as the working fluid of solar collectors increases their outlet temperature. The average temperature difference of the PDC and FPC in Tehran when using water/MWCNT nanofluid instead of water are increased by 1.96 and 0.79 degrees, respectively. These values in Beijing are 1.01 and 0.54 degrees for PDC and FPC, respectively. Moreover, the mean temperature difference of the PDC and FPC in Tehran when using Dowtherm Q /MWCNT nanofluid instead of Dowtherm Q are increased by 1.03 and 0.42 degrees, respectively. These values in Beijing are 0.53 and 0.29 degrees for PDC and FPC, respectively. Therefore, the use of nanofluids as a new medium for heat transfer can have a significant effect on increasing the rate of heat transfer, consequently leading to improved solar collector performance.

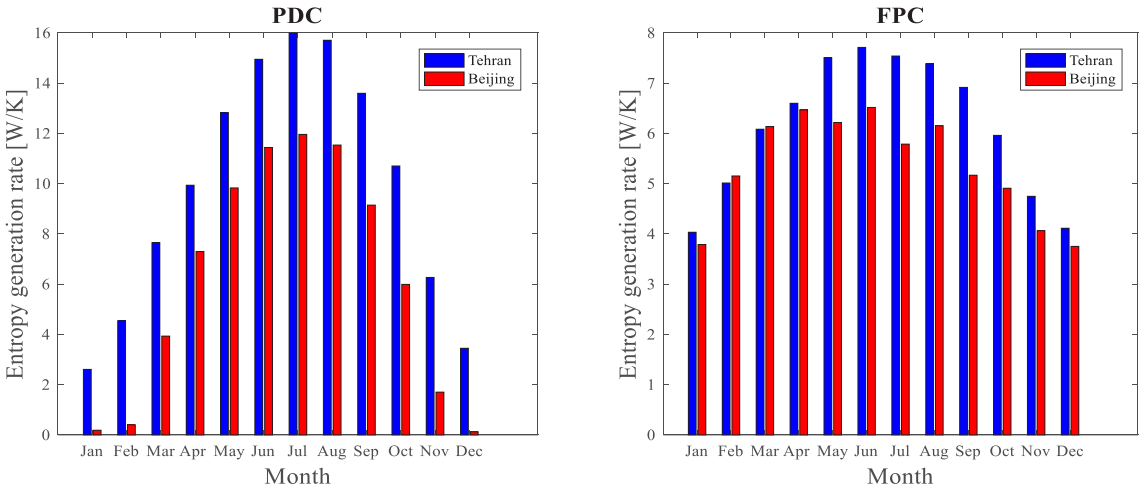

Fig. 9. Monthly average entropy generation rate of PDC (left) and FPC (right) in selected regions.

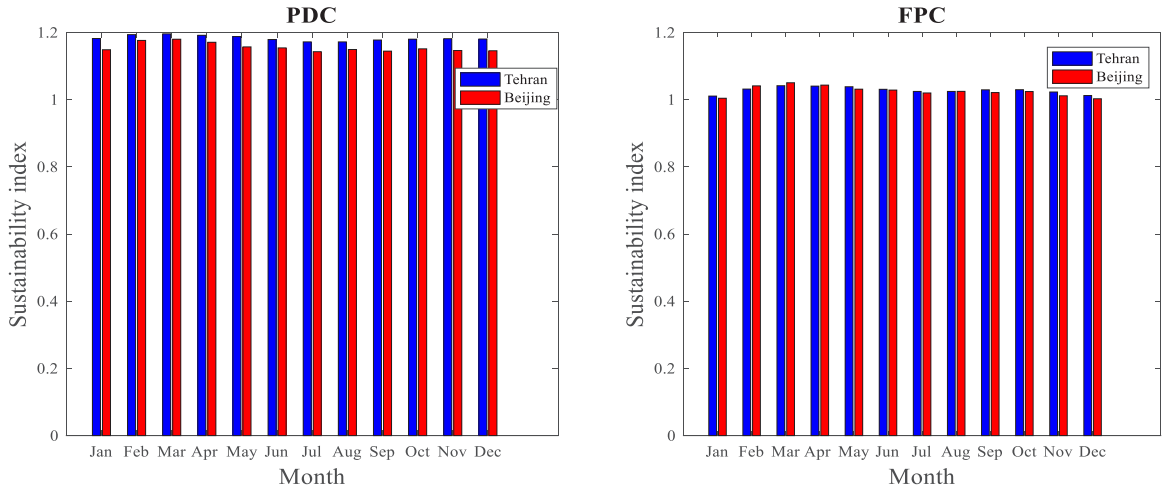

Fig. 10. Monthly average sustainability index of PDC (left) and FPC (right) in selected regions.

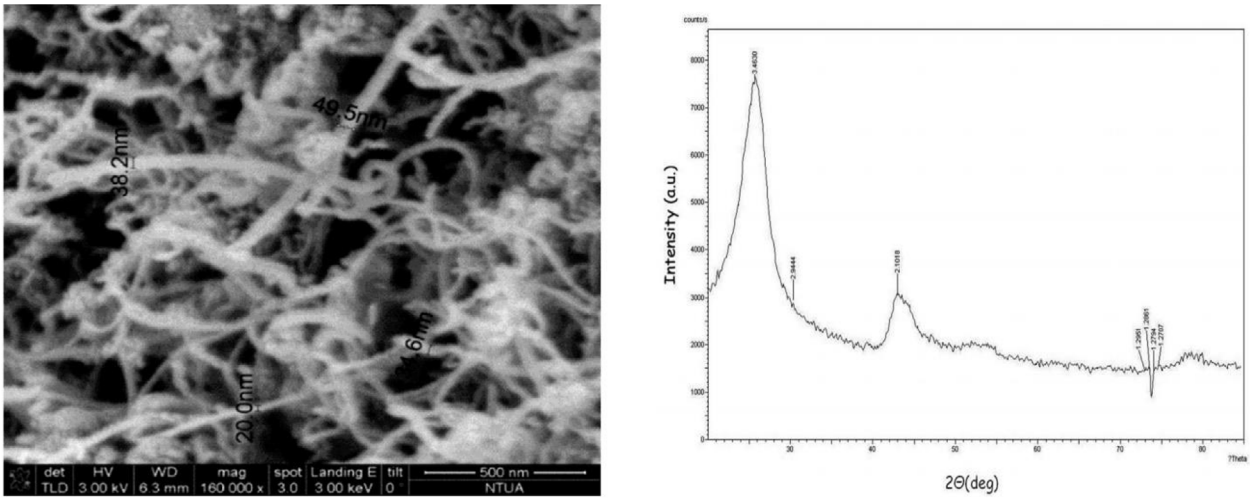

Fig. 11. (a) SEM image and (b) XRD graph of MWCNT particles (Asadi et al., 2019; Kyriakidou et al., 2020).

Table 5
The temperature difference (in degree) of PDC and FPC with different heat transfer fluids in selected regions.

Month	Jan	Feb	Mar	Apr	May	Jun	Jul	Aug	Sep	Oct	Nov	Dec
PDC												
W (T)	9.68	12.82	16.27	17.95	20.92	21.59	21.03	20.53	18.98	15.87	11.97	9.93
D (T)	5.07	6.71	8.52	9.4	10.96	11.31	11.02	10.75	9.94	8.32	6.27	5.2
W+M (T)	10.83	14.34	18.21	20.09	23.41	24.16	23.53	22.97	21.24	17.76	13.39	11.12
D+M (T)	5.65	7.52	9.53	10.49	12.21	12.69	12.36	12.05	11.13	9.35	7.03	5.8
W (B)	5.02	8.02	10.21	10.95	10.39	11.06	9.43	10.25	8.06	7.48	5.63	4.94
D (B)	2.63	4.2	5.35	5.74	5.44	5.79	4.94	5.37	4.22	3.92	2.95	2.59
W+M (B)	5.62	8.98	11.42	12.25	11.62	12.38	10.55	11.47	9.02	8.38	6.3	5.53
D+M (B)	2.92	4.72	6.01	6.45	6.1	6.51	5.53	6.03	4.69	4.36	3.32	2.94
FPC												
W (T)	0.95	3.6	6.52	7.95	10.46	11.03	10.55	10.12	8.82	6.19	2.88	1.17
D (T)	0.5	1.89	3.42	4.16	5.48	5.78	5.53	5.3	4.62	3.24	1.51	0.61
W+M (T)	1.07	4.03	7.3	8.89	11.7	12.34	11.81	11.33	9.87	6.93	3.23	1.31
D+M (T)	0.56	2.12	3.81	4.66	6.16	6.46	6.21	5.94	5.19	3.61	1.69	0.68
W (B)	0.29	3.98	6.67	7.59	6.89	7.72	5.71	6.72	4.02	3.32	1.04	0.2
D (B)	0.15	2.09	3.49	3.97	3.61	4.04	2.99	3.52	2.11	1.74	0.54	0.1
W+M (B)	0.33	4.46	7.47	8.49	7.71	8.64	6.39	7.52	4.5	3.72	1.16	0.24
D+M (B)	0.17	2.34	3.9	4.46	4.05	4.54	3.34	3.94	2.37	1.94	0.61	0.13

W = Water, D = Dowtherm Q, M = MWCNT, T = Tehran, B = Beijing.

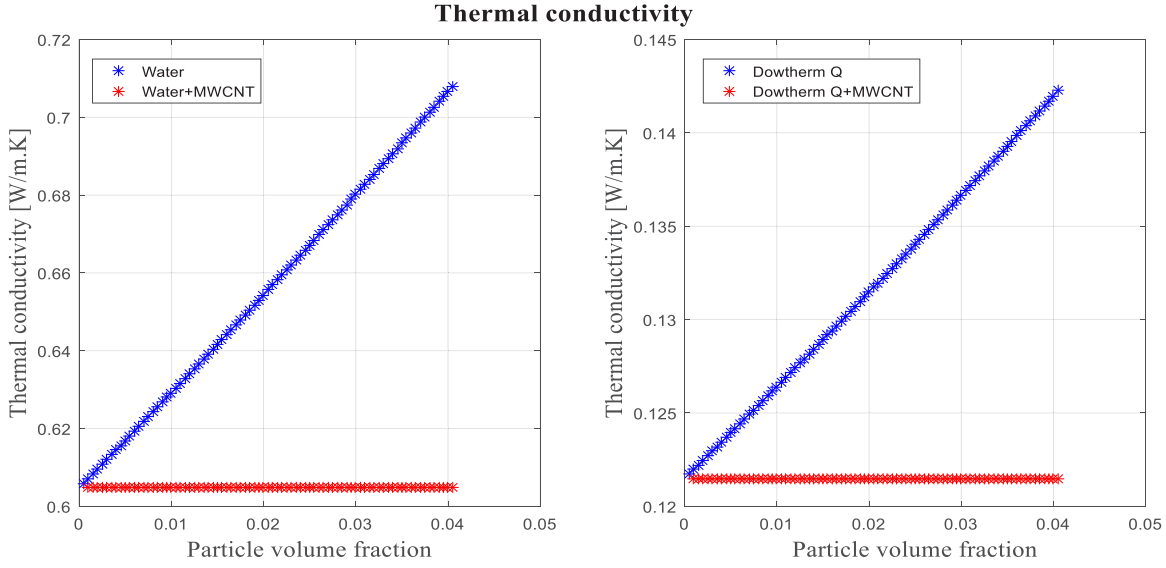

Fig. 12. Thermal conductivity of base fluids and nanofluids as a function of particle volume fraction.

4.4. Levelized cost of energy

Apart from the environmental benefits of using solar energy, which has significant benefits for human society, determining the LCOE of solar collectors can be beneficial to governments and investors. In addition, it is proven that the LCOE is the most commonly used indicator to assess the feasibility of solar collectors. The results of the LCOE calculation for FPC and PDC systems with various HTFs and nanofluids in Beijing and Tehran are given in Fig. 13. Note that the mean values of Q in Beijing and Tehran is used to calculate the LCOE. Furthermore, the interest rate, operation years and working hours of solar collectors are considered to 8%, 20 years and 6 h per day, respectively. According to Eq. (21), the LCOE decreases as the solar system useful output power increases and the purchase cost of collector decreases. The cost of flat plate collector less than that dish collector. However, the useful output power of the PDC is higher than that FPC, which leads to a lower LCOE of the PDC compared to that FPC. Fig. 13 revealed that in both cities the PDC is less LCOE than that FPC (for all heat transfer fluids and nanofluids). In addition, it was found that the lowest and highest LCOE are related to PDC (in Tehran with water) and FPC (in Beijing with Dowtherm Q), respectively.

Although the use of nanofluids improves the performance of solar collectors, the high price of nanoparticle leads to an increase in LCOE of solar collector when using nanofluids. For instance, for Tehran, LCOE of PDC increases more than 5.5-fold when using water/MWCNT nanofluid instead of water.

4.5. Enviroeconomic and exergoenviroeconomic

The enviroeconomic (E_1) assessment is provided as a tool to evaluate the solar collectors' carbon pricing. In addition, the exergoenviroeconomic (E_2) analysis assesses the amount of CO_2 emission. Fig. 14 provided the Enviroeconomic, and exergoenviroeconomic parameters of solar collectors in Tehran and Beijing. It was found that the value of both parameters is higher in Tehran than in Beijing. Because Tehran has a higher average solar intensity compared to Beijing. According to Eqs. (22) and (23), both Enviroeconomic and exergoenviroeconomic parameters are directly related to the amount of solar radiation (input solar energy). In addition, the value of these parameters is the same for both solar collectors. The average values of E_1 and E_2 in Tehran are 69.23% and 66.67% higher than in Beijing, respectively. In addition, the lowest values of E_1 and E_2 in Tehran are 0.0014 and 0.0013 $ per day, respectively, which is related to Jan. The lowest values of E_1 and E_2 in Beijing are 0.0009 and 0.0007 $ per day, respectively, which is related to Dec. Therefore, in general it can be concluded that the amount of d CO_2 released in Tehran is more than in Beijing.

4.6. Challenges of solar energy development

Solar energy has been considered by countries from two points of view. First, the sun is a free energy source, and if the infrastructure of this technology is provided, the use of solar electricity/heat will be very economical and market fluctuations or political and international factors will not interfere in its supply. Second, electricity or heat generated by sunlight is considered one of the cleanest types of energy, and gas power plants are not comparable to solar energy plants from this point of view. A country that can expand its solar infrastructure and grid faster will compete in electricity generation and economic development; because investing in solar energy means investing in energy independence. In 2016, China's National Energy Agency announced that China has become the world's largest solar energy producer. China is not only the most populous country in the world, but is now also the largest solar energy producer in the world. The same organization recently announced that in the first three months of 2020, 3.95 GW was added to the capacity of the country's solar power plants, of which about 56% are large-scale PV systems and the rest are DG and small-scale plants. Therefore, the total installed capacity of solar power plants in China has reached 208 GW by the end of March 2020. However, although this capacity is amazing, it is insignificant compared to the high population of China. The main challenges of further development of solar energy technology in China include some issues. The initial draft of China's 2020 solar policy has left the Chinese people skeptical about the possible budget for the solar power plant. Another challenge is the possibility of falling coal prices in China, which is a new threat to the development of solar power plants. In addition, China's air pollution is a major obstacle to solar power generation. Air pollution in China prevents sunlight from reaching the solar panel, which has significantly reduced energy production. Researchers from 2003 to 2014 in northern and eastern China, the most polluted parts of the country, found that energy production was reduced by up to 1.5kWh/m^2 per day due to pollution. In the East, production has fallen by up to 35%, while it has been one of the top 10 producers of solar energy in recent years. Research also shows that in western China; where industrialization and urbanization are not widespread and pollution is lower than in other regions, solar energy production has dropped by up to 10%. The worst time is in the winter, when in addition to pollution, the clouds also block sunlight, during which time solar energy production is reduced by about 20%.

Regarding Iran's capacity to develop solar energy, it should be noted that if a country like China can focus on solar energy, Iran has the potential to invest even more in the solar industry; because the number of sunny days in Iran is much more than in China. In most regions of Iran, there are about 300 sunny days a year, which reduces the need for quantitative expansion of solar power plants. According to the Iranian Ministry of Energy, the total capacity of Iran's solar energy has reached about 365 MW by the end of June 2020. Meanwhile, about 0.4% of the Iran's area has a power generation capacity of 170 W/m^2 and 17.3% of the Iran's area (equivalent to 28 million hectares), has a power generation capacity of 260 W/m^2. However, despite this high potential, no proper action has been taken to exploit solar energy in Iran. There are barriers and challenges in the development of solar energy systems in Iran electricity markets. One of the main challenges in Iran is the lack of micro-policies and regulatory programs over the development of such systems. Another important obstacle is the existence of oil and gas resources and the perception of the abundance of these resources in Iran. However, experts and officials believe that relying on fossil fuels, especially oil, could cause irreparable damage at the national level in the near future, especially for future generations. Therefore, it can be said that in Iran, considering the availability of fossil resources and the delivery of cheap fossil fuels to power plants and the transportation system, supporting the production of clean energy is still not one of the country's priorities in terms of energy supply. On the other hand, there are challenges in the purchase price of electricity generated by the Ministry of Energy, obtaining the necessary licenses from relevant institutions and creating the necessary incentives in the private sector for production. Unfortunately, one of the main problems in this field is the existence of vertical organizational structures with multiple layers in the country's organizations, lack of transparency and segregation of duties, and the existence of multitasking in many executive departments, which has delayed the development of solar energy systems. An example of overlap and parallelism in the structure of Iran's solar energy is the similar activities of the New Energy Organization of Iran and the Renewable Energy Technology Development Center. The priorities of the solar energy working group of these organizations are localization and gaining the capability of domestically built solar systems and sustainable development and improving security. However, one of the main problems currently facing the development of solar farms in Iran is the issue of finance and banking issues. That is, to work in the field of solar energy, it should be possible to borrow from banks. Since it is very difficult and complicated to get a loan in Iran to work in the field of energy, and on the other hand, the fees of banks in this field are very high and unusual, so the possibility of investment is very low. Foreign investors, who can borrow or lend from foreign banks, are also concerned about international problems due to recent international constraints, which have also slowed the development of such systems. Development of solar energy application in Iran, in addition to international obstacles, faces other national, local and regional problems. Some of the most important obstacles to the development of solar energy projects in Iran include the lack of policies and programs for development, lack of national and local laws about renewable energy, lack of awareness of planners and national managers with the use of this type of energy resources, weakness in human resource management and barriers to technology transfer have been identified

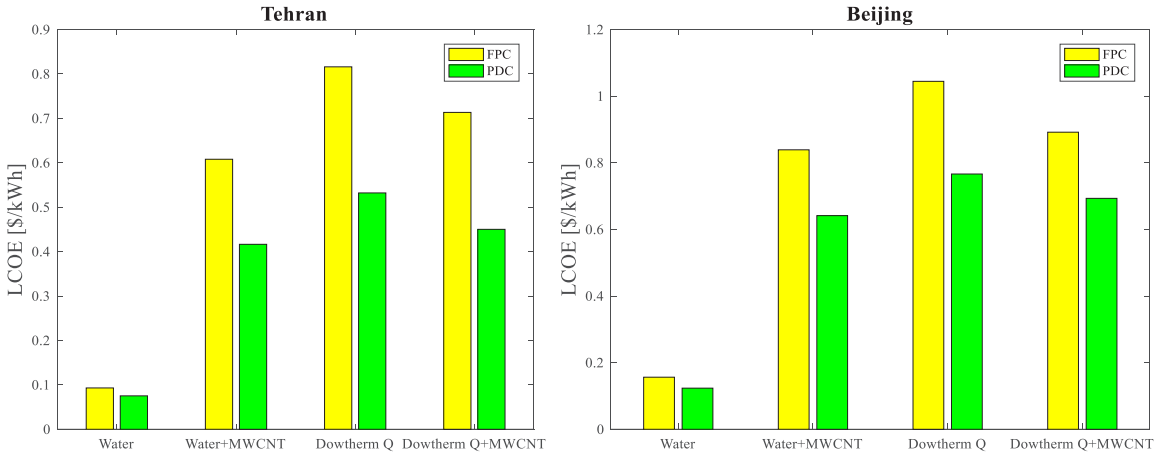

Fig. 13. LCOE for different solar collectors with different heat transfer fluids and nanofluids in Tehran (left), and Beijing (right).

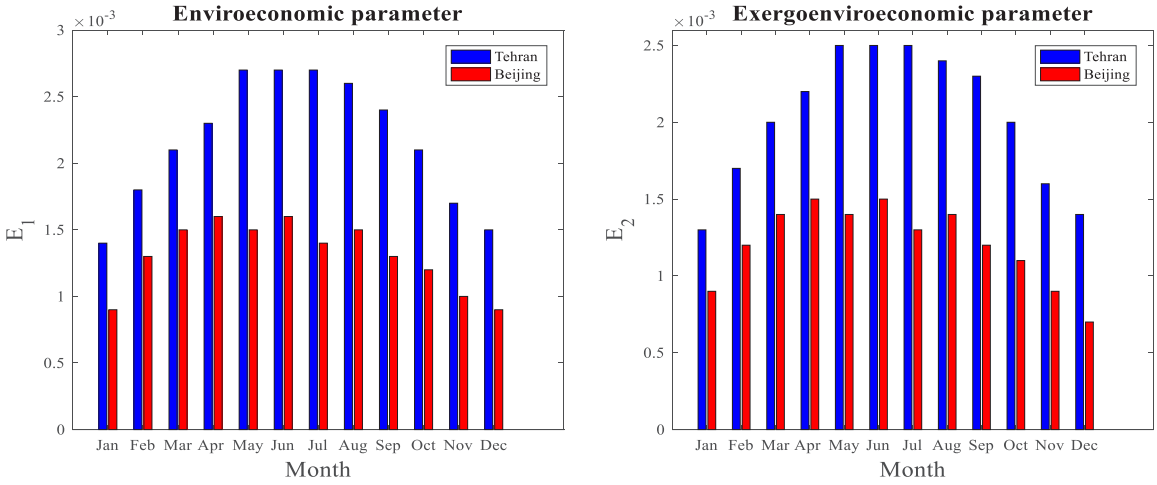

Fig. 14. Enviroeconomic (left), and exergoenviroeconomic (right) parameters of solar collectors in selected regions.

and investigated. Finally, there are undoubtedly other problems and challenges in this regard. But in general, any policy regarding the development of technologies for the production of renewable energy and their use should consider the market situation (customers and stakeholders of this technology), human resources (sufficient skilled manpower), primary resources, equipment and other infrastructure and technologies.

5. Conclusions

The use of conventional fuels has two major problems: depletion of reserves and air pollution. The future of energy demands for human society is related to renewable energy. Meanwhile, solar energy is one of the most common renewable sources of electricity and heat generation that has attracted of the world. However, the operation of solar energy systems is associated with some challenges and obstacles. The aim of this paper is to investigate and comparison two stationary and concentrating solar collectors of energy and exergy points of view. In this work, the performance of two FPC and PDC systems in Tehran and Beijing are investigated. The influence of using different fluids as well as nanofluids as a HTF on performance solar thermal systems is examined. In addition, parameters such as LCOE, Enviroeconomic (E_1) and Exergoenviroeconomic (E_2), SI and S_g for solar systems are investigated and compared. The main objectives of this work are to comprehensively study the performance of two types of solar collectors for thermal energy generation and compare them in Tehran and Beijing, decreasing the consumption of fossil fuel and so decrement emissions of pollutants by use of solar energy and ability to apply the obtained results for use in experimental works. Furthermore, the obstacles and challenges of solar energy development in Iran and China are discussed. The main results are as follows:

- The average useful output power of the PDC and FPC in Tehran is 94.7% and 48.1% higher than that in Beijing, respectively. In addition, in both regions, the highest energy efficiency of the PDC and FPC is related to the Jun;
- In both regions, the PDC has better energy performance compared to the FPC. In other words, to provide the certain thermal energy, a smaller area of the PDC is required compared to the FPC;
- In the months when the solar collector has lower exergy efficiency, its use in Tehran compared to that Beijing has a better exergy performance than other months;
- The PDC system in Tehran has more potential to generate entropy. Furthermore, the average SI rate of PDC in Tehran and Beijing is 15.06% and 12.71% higher than the value in the FPC system, respectively;
- In both cities the PDC is less LCOE than that FPC (for all HTFs and nanofluids). In addition, the lowest and highest LCOE are belong to PDC (in Tehran with water) and FPC (in Beijing with Dowtherm Q), respectively;
- The use of nanofluids as a new medium for heat transfer can have a significant effect on increasing the rate of heat

transfer, consequently leading to improved solar collectors performance;
- For Tehran, LCOE of PDC increases more than 5.5-fold when using water/MWCNT nanofluid instead of water;
- The average values of E_1 and E_2 in Tehran are 69.23% and 66.67% higher than in Beijing, respectively;
- The total installed capacity of solar power plants in China has reached 208 GW by the end of March 2020. However, although this capacity is amazing, it is insignificant compared to the high population of China;
- Development of solar energy application in Iran, in addition to international obstacles, faces other national, local and regional problems.

Future works could examine the performance of solar collectors with other energy systems such as ORC, thermionic and thermoelectric generators, reformer, etc. Also, they can be used in gas turbine-based cycles, fuel cells and biomass. Overall, the obtained results of present paper and challenges raised are very encouraging and useful for governments and energy systems engineers and designers.

CRediT authorship contribution statement

Ping Ouyang: Conceptualization, Formal analysis, Investigation, Methodology, Software, Writing - original draft, Writing - review & editing. **Yi-Peng Xu:** Conceptualization, Investigation, Methodology, Software, Writing - original draft, Writing - review & editing. **Lu-Yu Qi:** Conceptualization, Investigation, Methodology, Software, Writing - original draft, Writing - review & editing. **Si-Ming Xing:** Conceptualization, Investigation, Methodology, Software, Writing - original draft, Writing - review & editing. **Hadi Fooladi:** Conceptualization, Investigation, Methodology, Software, Writing - original draft, Writing - review & editing.

Declaration of competing interest

The authors declare that they have no known competing financial interests or personal relationships that could have appeared to influence the work reported in this paper.

Acknowledgments

This project was funded by the Project of Technology Innovation and Application Demonstration of Chongqing (cstc2018jscx-msybX0339), Science and Technology Research Program of Chongqing Municipal Education Commission (KJQN201800822, KJQN201800816, KJZD-K201800801 and KJZD-M201900802).

References

Abuşka, M., Şevik, S., 2017. Energy, exergy, economic and environmental (4E) analyses of flat-plate and V-groove solar air collectors based on aluminium and copper. Sol. Energy 158, 259–277.
Aghajani, G., Ghadimi, N., 2018. Multi-objective energy management in a micro-grid. Energy Rep. 4, 218–225.
Agyekum, E.B., Velkin, V.I., 2020. Optimization and techno-economic assessment of concentrated solar power (CSP) in South-Western Africa: A case study on Ghana. Sustain. Energy Technol. Assess. 40, 100763.
Ahmadi, M.H., et al., 2013. Designing a solar powered stirling heat engine based on multiple criteria: maximized thermal efficiency and power. Energy Convers. Manage. 75, 282–291.
Algieri, A., et al., 2020. Analysis of multi-source energy system for small-scale domestic applications. Integration of biodiesel, solar and wind energy. Energy Rep. 6, 652–659.
Araújo, K., Boucher, J.L., Aphale, O., 2019. A clean energy assessment of early adopters in electric vehicle and solar photovoltaic technology: Geospatial, political and socio-demographic trends in New York. J. Cleaner Prod. 216, 99–116.
Asadi, A., et al., 2019. An experimental investigation on the effects of ultrasonication time on stability and thermal conductivity of MWCNT-water nanofluid: Finding the optimum ultrasonication time. Ultrason. Sonochem. 58, 104639.
Bagal, H.A., et al., 2018. Risk-assessment of photovoltaic-wind-battery-grid based large industrial consumer using information gap decision theory. Sol. Energy 169, 343–352.
Barbosa, E.G., et al., 2020. Experimental evaluation of a stationary parabolic trough solar collector: Influence of the concentrator and heat transfer fluid. J. Cleaner Prod. 276, 124174.
Barreto, G., Canhoto, P., 2017. Modelling of a Stirling engine with parabolic dish for thermal to electric conversion of solar energy. Energy Convers. Manage. 132, 119–135.
Beltrán-Chacon, R., et al., 2015. Design and analysis of a dead volume control for a solar stirling engine with induction generator. Energy 93, 2593–2603.
Bhowmik, H., Amin, R., 2017. Efficiency improvement of flat plate solar collector using reflector. Energy Rep. 3, 119–123.
Boukelia, T., Arslan, O., Mecibah, M., 2016. ANN-based optimization of a parabolic trough solar thermal power plant. Appl. Therm. Eng. 107, 1210–1218.
Cai, W., et al., 2019. Optimal bidding and offering strategies of compressed air energy storage: A hybrid robust-stochastic approach. Renew. Energy 143, 1–8.
Caliskan, H., 2015. Thermodynamic and environmental analyses of biomass, solar and electrical energy options based building heating applications. Renew. Sustain. Energy Rev. 43, 1016–1034.
Caliskan, H., 2017. Energy, exergy, environmental, enviroeconomic, exergoenvironmental (EXEN) and exergoenviroeconomic (EXENEC) analyses of solar collectors. Renew. Sustain. Energy Rev. 69, 488–492.
Caliskan, H., Dincer, I., Hepbasli, A., 2012. Exergoeconomic, enviroeconomic and sustainability analyses of a novel air cooler. Energy Build. 55, 747–756.
Charalambous, P., et al., 2011. Optimization of the photovoltaic thermal (PV/T) collector absorber. Sol. Energy 85 (5), 871–880.
Chen, Z., et al., 2012. Efficiencies of flat plate solar collectors at different flow rates. Energy Procedia 30, 65–72.
Cheng, S., et al., 2020. A new hybrid solar photovoltaic/phosphoric acid fuel cell and energy storage system; Energy and Exergy performance. Int. J. Hydrogen Energy.
Cherif, H., et al., 2019. A receiver geometrical details effect on a solar parabolic dish collector performance. Energy Rep. 5, 882–897.
Deng, J., et al., 2016. Dynamic thermal performance prediction model for the flat-plate solar collectors based on the two-node lumped heat capacitance method. Sol. Energy 135, 769–779.
Diez, F., et al., 2019. Modelling of a flat-plate solar collector using artificial neural networks for different working fluid (water) flow rates. Sol. Energy 188, 1320–1331.
Ehyaei, M., et al., 2019. Energy, exergy and economic analyses for the selection of working fluid and metal oxide nanofluids in a parabolic trough collector. Sol. Energy 187, 175–184.
Fan, X., et al., 2020. Multi-objective optimization for the proper selection of the best heat pump technology in a fuel cell-heat pump micro-CHP system. Energy Rep. 6, 325–335.
Fudholi, A., et al., 2019. Exergy and sustainability index of photovoltaic thermal (PVT) air collector: A theoretical and experimental study. Renew. Sustain. Energy Rev. 100, 44–51.
Gavagnin, G., et al., 2017. Cost analysis of solar thermal power generators based on parabolic dish and micro gas turbine: Manufacturing, transportation and installation. Appl. Energy 194, 108–122.
Hafez, A., et al., 2016. Solar parabolic dish stirling engine system design, simulation, and thermal analysis. Energy Convers. Manage. 126, 60–75.
Hamian, M., et al., 2018. A framework to expedite joint energy-reserve payment cost minimization using a custom-designed method based on mixed integer genetic algorithm. Eng. Appl. Artif. Intell. 72, 203–212.
Huang, W., Marefati, M., 2020. Energy, exergy, environmental and economic comparison of various solar thermal systems using water and Thermia Oil B base fluids, and CuO and Al_2O_3 nanofluids. Energy Rep. 6, 2919–2947.
Kalogirou, S.A., 2013. Solar Energy Engineering: Processes and Systems. Academic Press.
Karimi, R., Gheinani, T.T., Avargani, V.M., 2019. Coupling of a parabolic solar dish collector to finned-tube heat exchangers for hot air production: An experimental and theoretical study. Sol. Energy 187, 199–211.
Khanjari, Y., Pourfayaz, F., Kasaeian, A., 2016. Numerical investigation on using of nanofluid in a water-cooled photovoltaic thermal system. Energy Convers. Manage. 122, 263–278.
Khwayyir, H.S., Baqir, A.S., Mohammed, H.Q., 2020. Effect of air bubble injection on the thermal performance of a flat plate solar collector. Therm. Sci. Eng. Prog. 17, 100476.
Kyriakidou, K., et al., 2020. In vitro cytotoxicity assessment of pristine and carboxyl-functionalized MWCNTs. Food Chem. Toxicol. 141, 111374.
Li, H., et al., 2020. Research on the policy route of China's distributed photovoltaic power generation. Energy Rep. 6, 254–263.
Liu, S., et al., 2020. Energy analysis using carbon and metallic oxides-based nanomaterials inside a solar collector. Energy Rep. 6, 1373–1381.

Loni, R.a., et al., 2017. Thermodynamic analysis of a solar dish receiver using different nanofluids. Energy 133, 749–760.
Loni, R., et al., 2018. Thermal and exergy performance of a nanofluid-based solar dish collector with spiral cavity receiver. Appl. Therm. Eng. 135, 206–217.
M., Hosseini Firouz, Ghadimi, N., 2016. Optimal preventive maintenance policy for electric power distribution systems based on the fuzzy AHP methods. Complexity 21 (6), 70–88.
Marefati, M., Mehrpooya, M., 2019. Introducing and investigation of a combined molten carbonate fuel cell, thermoelectric generator, linear fresnel solar reflector and power turbine combined heating and power process. J. Cleaner Prod. 240, 118247.
Marefati, M., Mehrpooya, M., Shafii, M.B., 2018. Optical and thermal analysis of a parabolic trough solar collector for production of thermal energy in different climates in Iran with comparison between the conventional nanofluids. J. Cleaner Prod. 175, 294–313.
Marefati, M., Mehrpooya, M., Shafii, M.B., 2019. A hybrid molten carbonate fuel cell and parabolic trough solar collector, combined heating and power plant with carbon dioxide capturing process. Energy Convers. Manage. 183, 193–209.
Mehrpooya, M., Marefati, M., 2020. Parametric design and performance evaluation of a novel solar assisted thermionic generator and thermoelectric device hybrid system. Renew. Energy.
Mehrpooya, M., Taromi, M., Ghorbani, B., 2019a. Thermo-economic assessment and retrofitting of an existing electrical power plant with solar energy under different operational modes and part load conditions. Energy Rep. 5, 1137–1150.
Mehrpooya, M., et al., 2019b. Solar fuel production by developing an integrated biodiesel production process and solar thermal energy system. Appl. Therm. Eng. 114701.
Meteotest, 2000. Weather data for every place on Earth. Available from: https://meteonorm.com/en/. [cited 5 April 2019].
Mohamed, M.M., Mahmoud, N.H., Farahat, M.A., 2020. Energy storage system with flat plate solar collector and water-ZnO nanofluid. Sol. Energy 202, 25–31.
Mohammadi, A., Mehrpooya, M., 2018. Techno-economic analysis of hydrogen production by solid oxide electrolyzer coupled with dish collector. Energy Convers. Manage. 173, 167–178.
Mohammed, I.L., 2012. Design and development of a parabolic dish solar water heater. Int. J. Eng. Res. Appl. 2 (1), 822–830.
Moradi, M., Mehrpooya, M., 2017. Optimal design and economic analysis of a hybrid solid oxide fuel cell and parabolic solar dish collector, combined cooling, heating and power (CCHP) system used for a large commercial tower. Energy 130, 530–543.
Mukherjee, A., et al., 2020. Performance evaluation of an open thermochemical energy storage system integrated with flat plate solar collector. Appl. Therm. Eng. 115218.
Oyekale, J., Petrollese, M., Cau, G., 2020. Multi-objective thermo-economic optimization of biomass retrofit for an existing solar organic Rankine cycle power plant based on NSGA-II. Energy Rep. 6, 136–145.
Pavlovic, S., Bellos, E., Loni, R., 2018. Exergetic investigation of a solar dish collector with smooth and corrugated spiral absorber operating with various nanofluids. J. Clean. Prod. 174, 1147–1160.
Pavlovic, S., et al., 2017. Experimental investigation and parametric analysis of a solar thermal dish collector with spiral absorber. Appl. Therm. Eng. 121, 126–135.
Peng, M.Y.-P., et al., 2020. Energy and exergy analysis of a new combined concentrating solar collector, solid oxide fuel cell, and steam turbine CCHP system. Sustain. Energy Technol. Assess. 39, 100713.
Petela, R., 2003. Exergy of undiluted thermal radiation. Sol. Energy 74 (6), 469–488.
Sadeghi, G., et al., 2020. Energy and exergy evaluation of the evacuated tube solar collector using cu2o/water nanofluid utilizing ANN methods. Sustain. Energy Technol. Assess. 37, 100578.
Shariatzadeh, O.J., et al., 2015. Modeling and optimization of a novel solar chimney cogeneration power plant combined with solid oxide electrolysis/fuel cell. Energy Convers. Manage. 105, 423–432.
Stefanovic, V.P., et al., 2018. A detailed parametric analysis of a solar dish collector. Sustain. Energy Technol. Assess. 25, 99–110.
Tanaka, H., 2015. Theoretical analysis of solar thermal collector and flat plate bottom reflector with a gap between them. Energy Rep. 1, 80–88.
Tian, Z., et al., 2020. A quick measurement method for determining the incidence angle modifier of flat plate solar collectors using spectroradiometer. Sol. Energy 201, 746–750.
Tong, Y., et al., 2019. Energy and exergy comparison of a flat-plate solar collector using water, Al_2O_3 nanofluid, and CuO nanofluid. Appl. Therm. Eng. 159, 113959.
Yaqi, L., Yaling, H., Weiwei, W., 2011. Optimization of solar-powered stirling heat engine with finite-time thermodynamics. Renew. Energy 36 (1), 421–427.
Ye, H., et al., 2020. High step-up interleaved dc/dc converter with high efficiency. Energy Sources Part A: Recov. Utilization Environ. Eff. 1–20.
Yu, D., et al., 2020. Energy management of wind-PV-storage-grid based large electricity consumer using robust optimization technique. J. Energy Storage 27, 101054.
Zadeh, P.M., et al., 2015. Hybrid optimization algorithm for thermal analysis in a solar parabolic trough collector based on nanofluid. Energy 82, 857–864.